ECO-FRIENDLY SYNTHESIS AND PHYSICOCHEMICAL CHARACTERIZATION OF NANOHYDROXYAPATITE FOR ENHANCING THE LUBRICATING PROPERTIES OF PALM OIL

Sindhu R L *[a,b], Anandakumar V M [a,b], Sini Chandran [a,b], Vishal P V[c,d]

[a]Mahatma Gandhi College, Thiruvananthapuram, Kerala, India, 695004

[b]University of Kerala, Thiruvananthapuram, Kerala, India, 695034

[c]College of Engineering Thiruvananthapuram, Kerala, India, 695016

[d]A P J Abdul Kalam Technological University, Thiruvananthapuram, Kerala, India, 695016

*Corresponding Author – Sindhu R L.

Abstract

Vegetable oils are eco-friendly and sustainable alternatives to hazardous mineral oil-based lubricants. Palm oil is a promising vegetable oil showing good lubricating properties. However, its Coefficient of Friction (COF), wear characteristics, pour point, cloud point, flash point, fire point, and corrosive stability are to be enhanced. The lubricating properties of base oils can be improved by using nanoparticles as additives. In this work, hydroxyapatite nanoparticles are used as an additive to enhance all the lubricating properties of palm oil and are evaluated. The optimum concentration of hydroxyapatite nanoparticles in palm oil shows very good lubricating properties compared to pure palm oil. Hydroxyapatite is an eco-friendly biomaterial that has a wide variety of biomedical applications. The main objective of the study is to improve the coefficient of friction, wear characteristics, pour point, cloud point, flash point, fire point, and corrosive stability of palm oil by the addition of hydroxyapatite nanoparticles.

Keywords: Hydroxyapatite, Lubricating Property, Flash Point, Fire Point, Cloud Point, Pour Point.

1. Introduction

The world is currently grappling with a significant energy crisis characterized by the increasing demand for energy and the depletion of natural resources. This crisis has far-reaching economic, environmental, and social implications, necessitating urgent measures to enhance energy efficiency and conservation. One often overlooked but critical aspect contributing to energy waste is the friction and wear in mechanical systems. Understanding and mitigating this source of energy loss can play

a crucial role in addressing the energy crisis. Friction is the resistance to motion when two surfaces slide against each other. It is a major source of energy loss in mechanical systems. In engines, machinery, and transportation systems, friction converts a significant portion of useful energy into heat, which is then dissipated into the environment [1,20]. Wear refers to the gradual removal of material from surfaces in contact, leading to the deterioration of components. This not only reduces the efficiency of machinery but also necessitates frequent repairs and replacements, consuming additional resources and energy. In industrial processes, friction and wear can lead to substantial energy loss. For instance, in manufacturing up to 40% of energy consumption is attributed to overcoming friction. Improving lubrication and material technologies can reduce these losses. Vehicles, whether automobiles, trains, or airplanes, lose a significant amount of energy due to friction in engines, bearings, and other moving parts. Reducing friction can enhance fuel efficiency, leading to lower energy consumption and emissions. In power plants, frictional losses in turbines, pumps, and other equipments reduce overall efficiency. Minimizing these losses can enhance the amount of usable energy generated from a given amount of fuel [20]. Nanoparticles have emerged as a promising approach to enhance the efficacy of lubricating oils, leading to a considerable decrease in friction and wear. Different types of nanoparticles (NP) can be incorporated into various lubricating oils to create nano-lubricants [1,2]. These minuscule particles, which typically measure between 1 and 100 nanometers, possess distinctive physical and chemical characteristics that can be utilized to enhance lubrication. Nanoparticles can create a protective tribofilm on contacting surfaces, minimizing direct metal-to-metal contact. This layer acts as a barrier, lowering friction and preventing wear. Some nanoparticles have self-repairing properties. They can fill in the micro-cracks and surface irregularities, smoothing the contact surfaces and reducing the asperities that cause wear. Spherical nanoparticles can act like tiny ball bearings, providing a rolling effect between contact surfaces. This rolling mechanism further decreases friction and minimizes wear. Nanoparticles can also participate in chemical reactions with the lubricant or the surface materials, forming compounds that reduce friction or increase surface hardness. Nanoparticles can improve the lubricant's friction and wear properties [3]. The type of material, size, shape, and concentration of the nanoparticle affect the lubricating properties of the base oil [4,5,6]. At the optimum nanoparticle concentration, friction and wear properties are minimized [7]. The rise of bio-based, environmentally friendly lubricants

is drawing more focus because of the dwindling mineral oil reserves and the adverse effects of non-renewable petroleum products on the environment. Vegetable oils and synthetic oils present feasible options for use as bio-lubricants. They are eco-friendly and sustainable alternatives to hazardous mineral oil-based lubricants. Palm oil is a promising vegetable oil showing good lubricating properties. However, its wear characteristics, pour point, etc., are to be enhanced. The lubricating properties of base oils can be improved by using nanoparticles as additives.

Hydroxyapatite (HA) nanoparticles have garnered considerable interest in recent years because of their distinctive characteristics and diverse applications. Hydroxyapatite is a naturally occurring mineral variant of calcium apatite represented by the chemical formula $Ca_{10}(PO_4)_6(OH)_2$. It is the principal inorganic component of bone and teeth. Because of its excellent properties like biocompatibility, bioactivity, osteoconductivity, and thermal stability, it has a wide range of biological and industrial applications. It is commonly used as a material for implants in the regeneration of bone tissue, targeted drug delivery systems, orthopaedics, maxillofacial surgery, and dentistry, as well as in bioimaging applications [8]. However, the industrial applications of hydroxyapatite nanoparticles are less explored. In this study, the use of hydroxyapatite nanoparticles to improve the lubricant properties of palm oil is investigated. Its hexagonal structure provides excellent load-bearing capacity and resistance to wear. When hydroxyapatite nanoparticles are introduced into palm oil, they interact with the metal surfaces under tribological conditions (pressure, temperature, and shear forces). These interactions result in the development of a tribofilm on the surfaces in contact. This tribofilm serves as a protective layer, stopping direct contact between metals. It lowers the friction coefficient and reduces wear by soaking up stresses and distributing the load more uniformly across the surfaces. Hydroxyapatite nanoparticles can fill in the microscopic grooves and asperities on the metal surfaces. This micro-filling effect results in a smoother surface profile, reducing friction and wear by minimizing the surface roughness that contributes to mechanical resistance [7]. The presence of hydroxyapatite improves the thermal stability of the oil, maintaining its lubricating properties over a wider range of operating temperatures. Hydroxyapatite is inherently hard and durable, contributing to the anti-wear characteristics of the lubricant [7,12]. It helps to protect the metal surfaces from abrasive wear and reduces the overall material loss. By reducing friction and wear, hydroxyapatite nanoparticles help in prolonging the lifespan of mechanical

components. This leads to less frequent maintenance and replacement, saving costs and resources. Lower friction results in reduced energy consumption in machinery. This improves the overall efficiency of mechanical systems, contributing to energy savings and lower operational costs [21]. Palm oil is renewable and biodegradable, making it an environmentally friendly alternative to conventional mineral oils. The addition of hydroxyapatite nanoparticles enhances their performance without compromising their ecological benefits.

The aim of this study is to improve the lubricant properties of palm oil by adding hydroxyapatite nanoparticles and to determine the optimum concentration of hydroxyapatite. The hydroxyapatite nanoparticles are synthesized using the chemical precipitation method. The lubricant property of palm oil is evaluated for 0.02%, 0.04%, 0.05% & 0.07% of hydroxyapatite nanoparticles. The coefficients of friction (COF) and wear scar diameters (WSDs) are assessed using the four-ball tester tribometer using ASTMD4172 standards. The cloud point, pour point, flash point, and fire point, and the corrosive stability of the nano lubricant were also evaluated. This research is unique because it is the first time that the hydroxyapatite nanoparticles have been reported to improve the lubricating properties of palm oil.

2. Materials and Methods

2.1 Materials

The chemicals used in this experiment are Ca $(NO_3)_2 4H_2O$ and (NH_4) (Merck). To maintain pH, NH_4OH (99%) solution was used. All reagents were used as received. Palm oil for the experimental study is purchased from a local vendor.

2.2 Synthesis and characterization of nanohydroxyapatite

In this work, simple chemical precipitation is used to synthesize nanohydroxyapatite. Suitable concentrations of calcium nitrate and diammonium hydrogen phosphate solutions are prepared using deionized water such that the molar ratio of calcium to phosphorus is 1.67. A solution of diammonium hydrogen phosphate is gradually introduced to the calcium nitrate solution while continuously stirring with a magnetic stirrer. The pH of the calcium nitrate solution is then adjusted to 9 using ammonia solution. The resulting solution is stirred continuously for 1 hour and aged for 18 hours. The suspension obtained was centrifuged at a speed of 3000 rpm and

washed well with deionized water. The obtained precipitate was heated to 80 ºC for 16 hours in a hot air oven and was crushed to fine powder using an agate mortar [11-12].

The structural analysis of the synthesized powder was done by powder X-ray diffraction. The X-ray diffraction pattern of the powdered specimen is taken using Bruker D8 ADVANCE with DAVINCI instrument operating at 30 kV and 10 mA using Cu Kα radiation (λ=1.5418 Å). Diffraction patterns were obtained within the range of 10° to 79° with a step size of 0.02^0. The crystallite size, lattice parameters, unit cell volume, and crystallinity of the synthesized sample were assessed.

The functional groups found in the sample were determined through the FTIR spectrum analysis. The FTIR spectrum of the synthesized sample was recorded for a wave number range of 4000 to 400 cm^{-1}. The FTIR spectra of prepared samples were recorded by the Thermo Scientific Nicolet iS50 instrument and recorded using the KBr pellet technique.

The components in the sample were examined using EDX. The optical properties and band gap of the sample were determined by UV-Visible spectroscopy (Thermoscientific Nicolet iS50). The thermal properties were analyzed using thermogravimetric analysis (Perkin Elmer STA 8000).

2.3 Preparation of Nano Lubricants

The mixing of nanoparticles with palm oil is an important step to produce this nano-lubricant. Different amounts of hydroxyapatite nanoparticles were dispersed into palm oil. The even distribution of nanoparticles in base oil was a challenge, as these particles tend to group together and settle. To address this, the created suspensions underwent magnetic stirring followed by 30 minutes of ultrasound treatment to achieve a stable mixture. Consequently, the agglomeration effect is reduced when the forces of Brownian motion and Van der Waals intermolecular attraction in the suspensions surpass the repulsive forces [6]. In this study, different weight percentages of hydroxyapatite were added to palm oil (0.02%, 0.04%, 0.05% & 0.07%).

2.4 Evaluation of Lubricant Properties

2.4.1 Four-Ball Test

The tribological characteristics of palm oil and a blend of palm oil with HA nanoparticles were assessed following ASTM D-4172 standards. A Four-Ball tester (Fig. 1) from DUCOM was employed for this evaluation. The test involved four chromium steel balls, each with a diameter of 12.7mm and a hardness rating of 64 HRC on the Rockwell Hardness Scale. Following the ASTM D-4172 standard, the spindle speed was set to 1200 rpm, and a load of 392 N was applied. The test was performed for 3600 seconds at a temperature of 75ºC. [6,16]. Following the test, the wear scar diameters were measured using an optical microscope.

2.4.2 Flash and Fire point of optimum concentration

The flash and fire point of the optimum composition of HA in palm oil has been evaluated as per ASTM D 92 standards using the Cleveland Open Cup (COC) equipment [22]. These assessments are conducted to manage safety concerns related to base oils, as a lower flash point implies a higher fire risk. When oils are heated to high temperatures, they become flammable because they create a mix of oil vapor and oxygen from the air that can ignite. Consequently, raising the flash and fire points of lubricant oils can greatly enhance the safety of gas turbines by minimizing the chances of fire and explosion in high-temperature situations [18,19,22].

2.4.3 Cloud and Pour Point apparatus for optimal condition

For most mineral-based industrial lubricants, the pour point signifies the temperature at which paraffin molecules aggregate into a solid white mass, resulting in the oil losing all fluid characteristics [19,24]. Low-temperature fluidity is the most essential property for lubricants to perform in extremely cold environments. The cloud and pour point apparatus is initialized by powering it on and allowing the temperature to decrease to the pre-determined test value with a maximum achievable cooling of -30℃. The sample is then loaded into a test tube sealed with a holed rubber stopper through which a temperature sensor is inserted. Once the desired temperature is reached, the test tube containing the sample is introduced into the apparatus. The sample is periodically removed at increasing temperature intervals to assess the cloud point, followed by the pour point determination.

2.4.4 Corrosive Stability test for optimum condition

The corrosion stability of the modified palm oil was assessed following the ASTM D 130 standard[23]. The colour of the copper strip after the test is compared with the standard colour code as per ASTM D130/IP 154.

3. Results and Discussion

3.1 Characterization of Nanoparticles

The X-ray diffraction (XRD) pattern (Fig.2) of the sample can be attributed to the hexagonal crystal structure of hydroxyapatite (ICDD No. 09-0432). No additional peaks are found, which shows that the obtained powder is pure and only one phase is present. The crystallite size of the powder was determined using the Scherrer formula,

$$D = \frac{0.9\lambda}{\beta \cos\theta}$$

The broadened nature of diffraction peaks shows that the grain size of the sample was in the nanometre range. Using the Scherrer equation size is found to be 20.2 nm. The degree of crystallinity was calculated, and its value was 85.65 %. The d spacing for the most intense peak is found to be 2.822 Å, which matches that of a hexagonal system with a primitive lattice [13,14,17] (Table 1). The schematic representation of the hexagonal structure of hydroxyapatite using VESTA software is shown in Fig. 3. There are two calcium ion positions (Ca(I) and Ca(II)). A total of 18 ions are densely packed in the hexagonal structure. At each hexagonal vertex, a calcium ion will be surrounded by three hexagons. Furthermore, there is a hydroxyl ion at the center of each unit cell. The hydroxyl group remains in the center surrounded by three calcium ions in a hexagon to create a ring. These result in the creation of a “chord” to the structure, which accounts for many properties of hydroxyapatite. The void space in between two hexagons is occupied by three phosphate tetrahedra per unit cell. Due to the nature of the crystal structure of hydroxyapatite, the ions within HA are capable of being substituted. The cationic and anionic substitutions are about substitutions of the calcium, phosphate, and/or hydroxyl ions.

The characteristic absorption bands corresponding to phosphate, carbonate, and hydroxyl groups were observed, confirming the presence of hydroxyapatite in the FT-IR (Fig.4). The band at 961cm^{-1} corresponds to the symmetric stretching mode of the PO_4^{3-} group, while the band at 1021cm^{-1} is attributed to the asymmetric stretching

mode of the PO_4^{3-} group. The bending modes of the phosphate group were identified at 600 cm^{-1} and 560 cm^{-1}, both associated with the in-plane bending vibration of O–P–O within the PO_4^{3-} group. The band at 3248 cm^{-1} corresponds to the OH stretching vibration of adsorbed water, while the band at 630 cm^{-1} is due to the stretching vibration of OH^- ions. Additionally, the band at 1420 cm^{-1} is attributed to the asymmetric stretching of the CO_3^{2-} group. FT-IR analysis confirms the successful formation of hydroxyapatite, with no other phases detected in the synthesized sample [8,9,10].

UV visible spectrum of synthesized samples was taken using the Thermoscientific Nicolet iS50 instrument (Fig.5). According to Beer-Lambert law, absorbance is directly proportional to the absorption coefficient (α). The energy intercept of the curve in the plot of $(\alpha hv)^2$ vs hv gives the value of band gap energy. For pure hydroxyapatite, it is obtained as 5.1eV. This is in accordance with the available literature [10].

The thermal stability of nano-hydroxyapatite powder is evaluated by thermogravimetric analysis. The thermal analysis of the synthesized sample is done by a thermal analyzer (Perkin Elmer STA 8000) over a temperature range of 30 ^{0}C - 800 ^{0}C (Fig. 6). Three stages of degradation as a result of absorbed and lattice water removal and de-hydroxylation of nano-hydroxyapatite were observed. These stages occur at 25-200 ^{0}C, 200–650 ^{0}C and 700 – 850^{0}C, respectively. The first stage is due to the loss of adsorbed water, and the second stage is due to the loss of structural water and due to decomposition of HPO_4^{2-}. In the third stage [12], decomposition of carbonate into CO_2 gas occurs. The TG curve of pure hydroxyapatite shows the weight loss during the examined temperature range. As illustrated in Fig. 8, a significant weight loss was observed up to approximately 400℃, primarily due to the removal of adsorbed and lattice water [13]. Beyond 550℃, the loss of carbonate ions may contribute to the overall weight reduction. The vaporization of lattice water, along with the dehydration and condensation of HPO_4^{2-}, occurs progressively up to 600 ℃ [11,12]. The total mass loss recorded up to 800 ℃ was 8.353%.

The morphology of nanohydroxyapatite was examined using transmission electron microscopy (Jeol/JEM 2100*)* with an accelerating voltage of 200 kV. HRTEM images (Fig. 7a and 7b) show that the particles were rod-shaped and tended to form

agglomerates. The mean particle size obtained from TEM analysis was 22.902 nm (Fig. 7c).

The elemental analysis of the synthesized powder was determined using energy-dispersive X-ray spectroscopy (Carl Zeiss EVO 18 Research), as shown in Fig.8. The Ca/P ratio obtained from EDX analysis is 1.77, which is closer to the expected value.

3.2 Lubricating property evaluation of a mixture of HA and palm oil

Friction and wear tests were performed using a four-ball wear test machine at varying concentrations of hydroxyapatite dispersed in 100 mL of palm oil. The coefficient of friction (COF) values obtained under these conditions are presented in Table 2, following the test parameters of 392 N, 1200 r/min, 75℃, and a duration of 60 minutes, as per ASTM D 4172 standards. The results indicate that COF decreases at lower concentrations of hydroxyapatite, which can be attributed to surface mending, the formation of a protective film, surface polishing, and the transition from sliding friction to rolling friction [2]. The minimum COF value was observed at a hydroxyapatite concentration of 0.04%. However, as the concentration of hydroxyapatite nanoparticles increased beyond this point, COF exhibited an increasing trend, likely due to nanoparticle agglomeration at higher concentrations [2,15]. Similarly, the wear scar diameter was smallest at a hydroxyapatite concentration of 0.04% by weight, but it increased with a further increase in concentration. The wear scar diameter decreases because the nanoparticles act as ball bearings between the surfaces in contact [25]. The increase is attributed to agglomeration, where larger aggregates form and fail to fit into the valleys between asperities effectively. As a result, they behave exactly like debris particles, causing wear that is abrasive in nature [2,15]. The coefficient of friction and wear scar diameter obtained from these experiments are plotted in Fig. 9and Fig. 10.

Figure - 11 illustrates the wear scar observed using a scar view microscope for a palm oil sample and Figure - 12 for a sample containing 0.04% HA in palm oil tested on a Four-Ball Tester. The figure displays three distinct types of wear scar images. Wear scar diameter is found to be minimum for 0.04 % of hydroxyapatite nanoparticles in palm oil. This is because these particles can form a protective tribofilm, act as rolling elements, and fill surface asperities. This makes them a promising biocompatible,

environmentally friendly alternative for advanced lubrication applications [15,19]. Due to the lowest wear values observed during testing, 0.04% concentration was selected as the optimum concentration of hydroxyapatite nanoparticles in palm oil.

The thermal properties of the palm oil with the optimum concentration of hydroxyapatite nanoparticles (0.04%) are evaluated and tabulated in Table 4. This sample has a higher fire point than pure palm oil, suggesting that it can function at higher temperatures. It can flow at lower temperatures because its pour point is lower than that of pure palm oil. It is evident that palm oil containing 0.04 weight percent hydroxyapatite nanoparticles can be utilized in a wide range of temperature conditions. Hydroxyapatite nanoparticles form a protective barrier, slowing the evaporation of lighter hydrocarbon fractions. Due to reduced vaporization, thermal stability, and non-flammable properties of nanohydroxyapatite nanoparticles flash point and fire point of palm oil increase. The introduction of nanoparticles causes wax crystal disruption, improved dispersion, and modification in viscosity, resulting in lower pour point and cloud point [20,21].

The corrosion test conducted on a solution containing 0.04% hydroxyapatite in 100 ml of palm oil was evaluated against the ASTM Copper Strip Corrosion Standards. The copper strip post-immersion exhibited a slight tarnish corresponding to a rating of 1a in Figure 13. This rating indicates a minimal level of corrosion characterized by barely discernible tarnish on the strip surface. The outcome suggests that the presence of hydroxyapatite at the given concentration has a negligible corrosive effect on copper when mixed with palm oil. This finding aligns with the ASTM standard for slight tarnish, confirming the protective potential of hydroxyapatite in such applications. The result is significant as it demonstrates the potential for using hydroxyapatite in oil formulations without causing detrimental corrosion to metal components. Due to the formation of a protective barrier, neutralization of acidic compounds, surface passivation, and water absorption and dispersion, hydroxyapatite nanoparticles can improve corrosive stability [25,26].

Conclusions

Hydroxyapatite nanoparticles are synthesized using the wet chemical precipitation method. Structural analysis was conducted using X-ray diffraction (XRD) and Fourier Transform Infrared (FTIR) spectroscopy. The optical properties of the sample were examined through UV-visible absorption spectroscopy, while its thermal characteristics were assessed using thermogravimetric analysis (TGA). The lubricating properties of palm oil for different concentrations of hydroxyapatite were evaluated (0 %, 0.02 %, 0.04 %, 0.05 % & 0.07 %). The optimum concentration of hydroxyapatite in palm oil for better lubricating properties was found to be 0.04 %. The COF for 0.04% of hydroxyapatite in palm oil was 11.11% lower than that of pure palm oil. The WSD shows a 13.72 % decrease, the pour point decreases from 20 ^{0}C to 4 ^{0}C, the cloud point decreases from 10 ^{0}C to 9 ^{0}C, the fire point increases from 230 ^{0}C to 335 ^{0}C, and the flash point increases from 220 ^{0}C to 305 ^{0}C. The mixture also shows good corrosive stability. Hence, hydroxyapatite nanoparticles have great potential to improve the lubricating properties of palm oil.

Author contributions

Sindhu R L: Conceptualization, Investigation, Analysis, Writing - original draft, Anandakumar V M: Supervision, Writing - review & editing, Sini Chandran: Investigation, Writing - original draft, Vishal PV: Investigation.

Acknowledgments

The authors are thankful to the authorities of Sophisticated Analytical Instrumental Facilities (SAIF), Cochin University of Science and Technology, and CLIF, University of Kerala, for providing advanced instrumental and analytical facilities. The authors would like to thank the Principal, M.G. College, Thiruvananthapuram, and the Principal, College of Engineering Trivandrum, for providing the facilities for doing this research.

References

1. Wang B, Qiu F, Barber GC, Zou Q, Wang J, Guo S, Jiang Q (2022) Role of nano-sized materials as lubricant additives in friction and wear reduction: a review. Wear 204206:490–491. https://doi.org/10.1016/j.wear.2021.204206

2. Ufyand IE, Zhinzhilo VA, Burlakova VE (2019) Metal-containing nanomaterials as lubricant additives: state-of-the-art and future development. Friction 7(2):93–116. https://doi.org/10.1007/s40544-019-0261-y

3. Kotia A, Rajkhowa P, Rao GS, Ghosh SK (2018) Thermophysical and tribological properties of nanolubricants: a review. Heat Mass Transfer 54(11):3493–3508. https://doi.org/10.1007/s00231-018-2351-1

4. Gulzar M, Masjuki HH, Kalam MA, Varman M, Zulkifi NWM, Mufti RA, Zahid R (2016) Tribological performance of nanoparticles as lubricating oil additives. J Nanoparticle Research 18(8):223. https://doi.org/10.1007/s11051-016-3537-4

5 Liu X, Xu N, Li W, Zhang M, Chen L, Lou W, Wang X (2017) Exploring the effect of nanoparticle size on the tribological properties of SiO2 / polyalkylene glycol nanofluid under different lubrication conditions. Tribology International 109:467–472. https://doi.org/10.1016/j.triboint.2017.01.007

6. Birleanu C, Pustan M, Cioaza M, Molea A, Popa F, Contiu G (2022) Effect of TiO2 nanoparticles on the tribological properties of lubricating oil: an experimental investigation. Scientific Reports 12:5201. https://doi.org/10.1038/ s41598-022-09245-2

7. Kerni L, Raina A, Haq MIU (2019) Friction and wear performance of olive oil containing nanoparticles in boundary and mixed lubrication regimes. Wear 426–427:819–827. https://doi.org/10.1016/j.wear.2019.01.022

8. Vijay H. Ingole, Shubham S. Ghule, Tomaž Vuherer, Vanja Kokol, Anil V. Ghule, Mechanical Properties of Differently Nanostructured and High-Pressure Compressed Hydroxyapatite-Based Materials for Bone Tissue Regeneration, Minerals 2021, 11, 1390.; https://doi.org/10.3390/min11121390

9. Angela Altomare, Ernesto Mesto, Maria Lacalamita, Bujar Dida, Altin Mele, Elvira Maria Bauer, Massimo Puzone, Emanuela Tempesta, Davide Capelli, Dritan Siliqi, and Francesco Capitelli, Structural Characterization of Low-Sr-Doped Hydroxyapatite Obtained by Solid-State Synthesis, Crystals 2023, 13, 117. https:// doi.org/10.3390/cryst13010117

10. Md. Sahadat Hossain, Supanna Malek Tuntun, Newaz Mohammed Bahadur and Samina Ahmed, Enhancement of photocatalytic efficacy by exploiting copper doping in nano-hydroxyapatite for degradation of Congo red dye, RSC Adv., 2022, 12, 34080–34094. https://doi.org/10.1039/D2RA06294A

11. F. Miyaji, Y. Kono, Y. Suyama, Formation and structure of zinc-substituted calcium hydroxyapatite, Mater. Res. Bull. 40 (2005) 209–220. 10.1016/j.materresbull.2004.10.020.

12. Mônica Rufino Senra, Rafaella Barbosa de Lima, Diego De Holanda Saboya Souza, Maria de Fátima Vieira Marques, Sergio Neves Monteiro, Thermal characterization of hydroxyapatite or carbonated hydroxyapatite hybrid composites with distinguished collagens for bone graft, Journal of Materials Research and Technology, Volume 9, Issue 4, July–August 2020, Pages 7190-7200. https://doi.org/10.1016/j.jmrt.2020.04.089.

13. Sophie C. Cox, Parastoo Jamshidi, Liam M. Grover, Kajal K. Mallick, Preparation and characterization of nanophase Sr, Mg, and Zn substituted hydroxyapatite by aqueous precipitation, Materials Science and Engineering: C, Volume 35, 1 February 2014, Pages 106-114, https://doi.org/10.1016/j.msec.2013.10.015.

14. Ihsan Ullaha, Muhammad Ali Siddiquia, Sharafadeen Kunle Kolawolea, Hui Liua, Ji Zhanga, Ling Rena, Ke Yanga, Synthesis, characterization and in vitro evaluation of zinc and strontium binary doped hydroxyapatite for biomedical application, Ceramics International 46 (2020) 14448–14459, https://doi.org/10.1016/j.ceramint.2020.02.242

15. Ananthan D. Thampi , M.A. Prasanth , A.P. Anandu , E. Sneha , Baiju Sasidharan , S. Rani, The effect of nanoparticle additives on the tribological properties of various lubricating oils – Review, Materials Today: Proceedings, Volume 47, Part 15, 2021, Pages 4919-4924. https://doi.org/10.1016/j.matpr.2021.03.664

16. Edla Sneha, RB Akhil, Abhijith Krishna, S Rani S Anoop Kumar, Formulation of bio-lubricant based on modified rice bran oil with stearic acid as an anti-wear additive,

Proc IMechE Part J: J Engineering Tribology1–8© IMechE 2020, DOI: 10.1177/1350650120977381

17. V. Rodríguez-Lugo,T. V. K. Karthik,D. Mendoza-Anaya,E. Rubio-Rosas,L. S. Villaseñor Cerón,M. I. Reyes-Valderrama,E. Salinas-Rodríguez, Wet chemical synthesis of nanocrystalline hydroxyapatite flakes: effect of pH and sintering temperature on structural and morphological properties, rsos.royalsocietypublishing.org R. Soc. open sci. 5: 180962, https://doi.org/10.1098/rsos.180962

18. Siti Safiyah Nor Azman, Nurin Wahidah Mohd Zulkifli, Hassan Masjuki, Mubashir Gulzar, Rehan Zahid, Study of tribological properties of lubricating oil blend added with graphene nanoplatelets, J. Mater. Res., 2016 _ Materials Research Society 2016, https://doi.org/10.1557/jmr.2016.24.

19. E. Sneha, S. Rani, and M. Arif, “Evaluation of lubricant properties of vegetable oils as base oil for industrial lubricant,” in IOP Conference Series: Materials Science and Engineering, Institute of Physics Publishing, Oct. 2019. doi: 10.1088/1757-899X/624/1/012022.

20. J. Zhao, Y. Huang, Y. He, and Y. Shi, “Nanolubricant additives: A review,” Friction, vol. 9, no. 5, pp. 891–917, Oct. 2021, doi: 10.1007/s40544-020-0450-8.

21. Jiang, Z., Sun, Y., Liu, B. et al. Research progresses of nanomaterials as lubricant additives. Friction 12, 1347–1391 (2024). https://doi.org/10.1007/s40544-023-0808.

22. A. Abdelkhalik, H. Elsayed, M. Hassan, M. Nour, A. B. Shehata, and M. Helmy, “Using thermal analysis techniques for identifying the flash point temperatures of some lubricant and base oils,” Egyptian Journal of Petroleum, vol. 27, no. 1, pp. 131–136, Mar. 2018, doi: 10.1016/j.ejpe.2017.02.006.

23. Malinovic, A. Borkovic, and T. Djuricic, “Copper strip corrosion testing in hydrocracked base oil in the presence of different inhibitors,” Hem Ind, vol. 76, no. 3, pp. 159–166, 2022, doi: 10.2298/HEMIND220113012M.

24. E. O. Eyankware, W. C. Ulakpa, and M. O. Eyankware, “Determination of cloud and pour point of crude oil with reference to crude transportation,” *Int. J. Sci. Healthc. Res.*, vol. 1, no. 3, pp. 20–25, 2016.

25. Q. He, A. Li, Z. Wang, Y. Zhang, L. Kong, and K. Yang, “Tribological behavior of ZnO-Si 3 N 4 nanoparticles-based lubricating grease,” J Exp Nanosci, vol. 13, no. 1, pp. 231–244, Jan. 2018, doi: 10.1080/17458080.2018.1511923.

26. Ndabezinhle Ngubhe Dube, Marwa ElKady, Hussien Noby, MohamedG.A. Nassef, Developing a sustainable grease from jojoba oil with plant waste based nano additives for enhancement of rolling bearing performance, Scientific Reports (2024) 14:539 | https://doi.org/10.1038/s41598-023-50003-9

Tables with legends

1. Table 1: The crystallite size, lattice constants, unit cell volume, and crystallinity of hydroxyapatite nanoparticles

Sample	Crystallite Size (nm)	Lattice Constants		Cell Volume ($Å^3$)	Crystallinity (%)
		a (Å)	c (Å)		
HA	20.2	9.4589	6.7160	520.3799	85.65

2. Table 2: The coefficient of friction for different weight percentages of hydroxyapatite nanoparticles

Wt.% of nanohydroxyapatite	COF
0	0.072±0.002
0.02 %	0.067±0.003
0.04 %	0.064±0.002
0.05 %	0.072±0.001
0.07 %	0.073±0.003

3. Table 3: The wear scar diameter for different weight percentages of hydroxyapatite nanoparticles

Wt.% of nanohydroxyapatite	**Wear (µm)**
0	729 ± 6
0.02 %	654 ± 5
0.04 %	629 ± 8
0.05 %	672 ± 7
0.07 %	704 ± 12

4. Table 4: The flash point, fire point, cloud point, and pour point for palm oil and palm oil with 0.04 % hydroxyapatite nanoparticles

Name of the Oil	**Flash Point (ºC)**	**Fire Point (ºC)**	**Cloud Point (ºC)**	**Pour Point (ºC)**
Pure Palm Oil	220	230	10	20
0.04% HA Palm oil	305	335	9	4

Figures with legends

1.

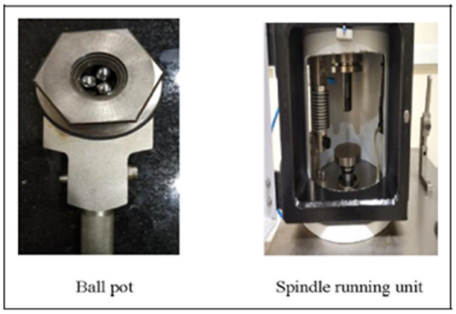

Fig. 1 – Four-Ball tester

2.

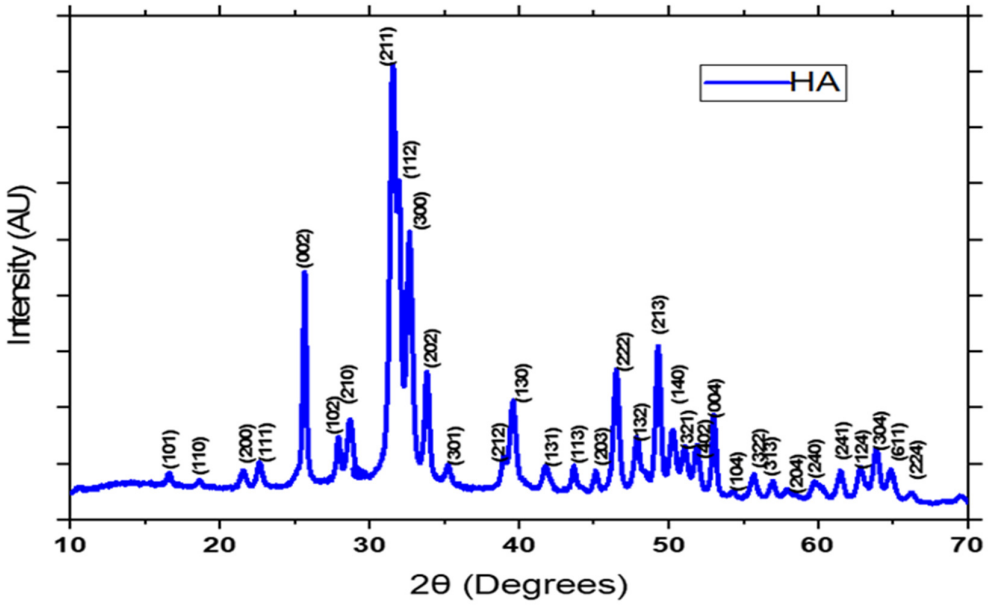

Fig. 2 – XRD pattern of hydroxyapatite nanoparticles

3.

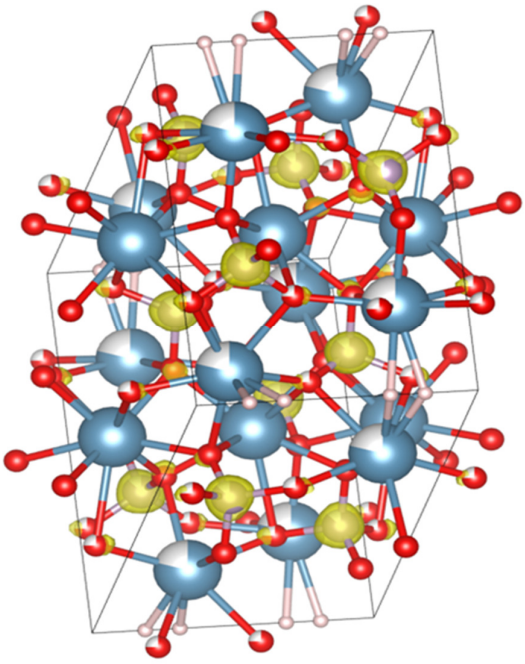

Fig. 3 – Structure of hydroxyapatite

4.

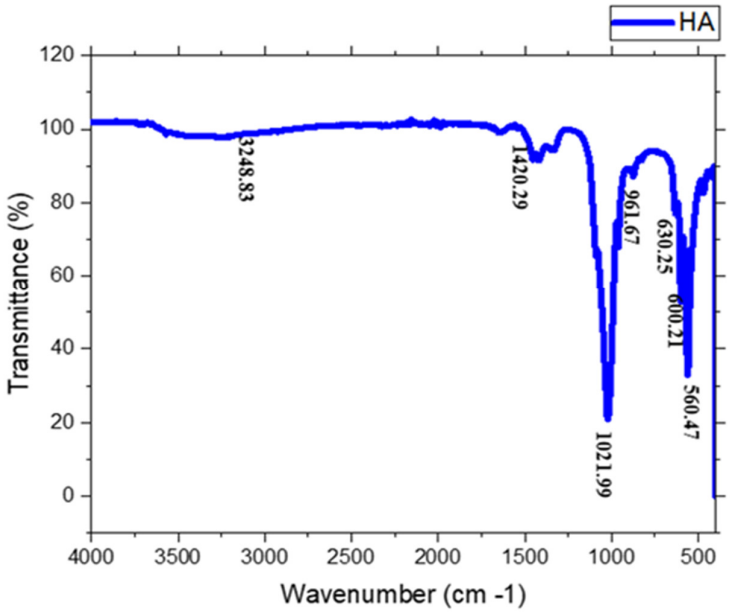

Fig. 4 – FT-IR spectrum of hydroxyapatite nanoparticles

5.

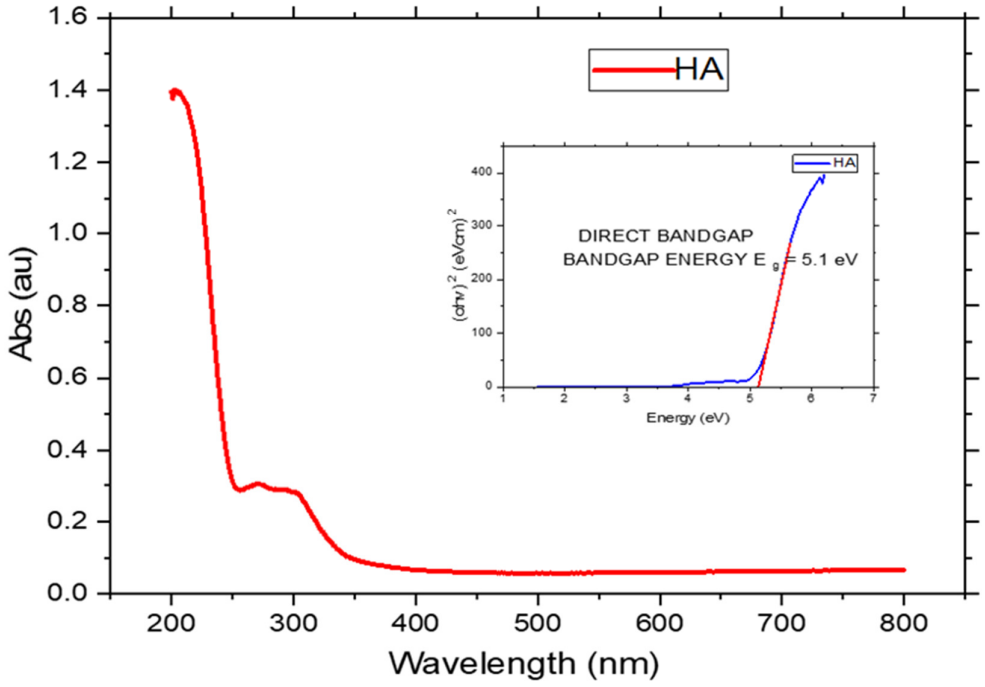

Fig. 5 – UV–Visible spectrum of hydroxyapatite nanoparticles

6.

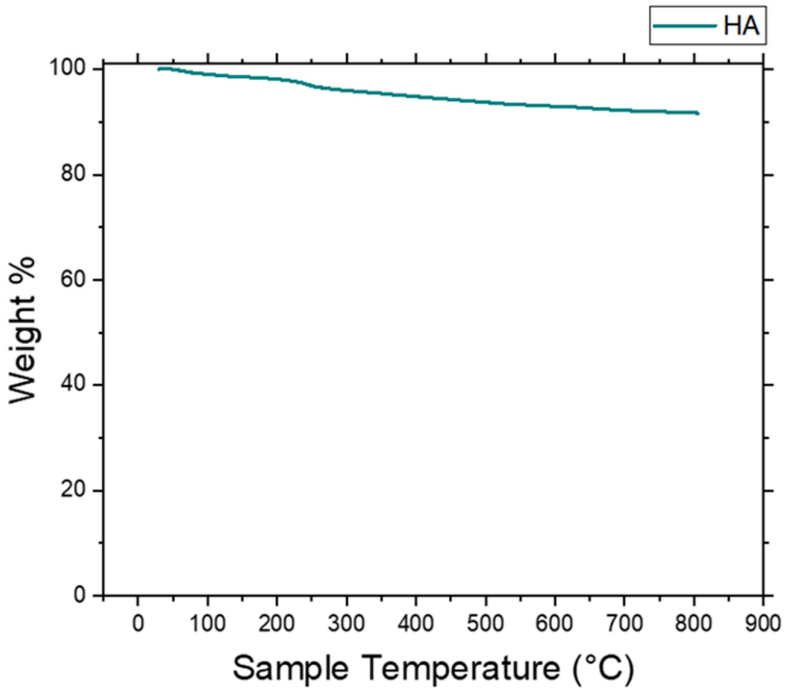

Fig. 6 – Thermogra□imetric cur□e of hydroxyapatite nanoparticles

7.

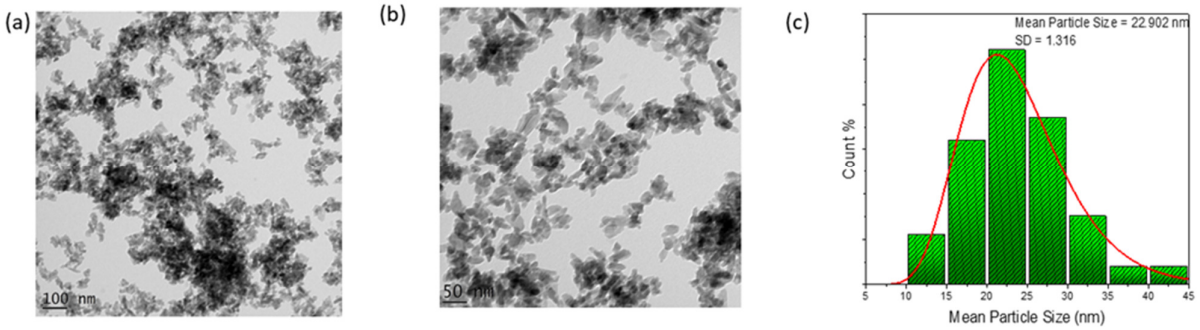

Fig. 7a & b – HRTEM image of hydroxyapatite nanoparticles, Fig. 7c – Particle size distribution

8.

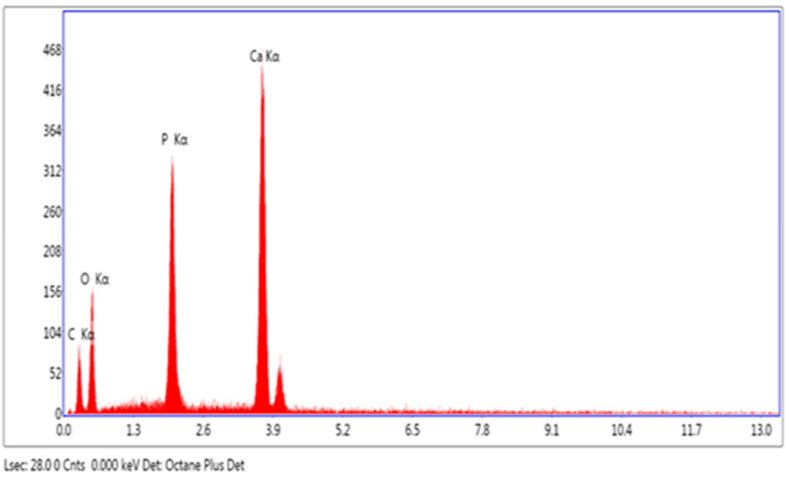

Fig. 8 – EDX spectrum of hydroxyapatite nanoparticles

9.

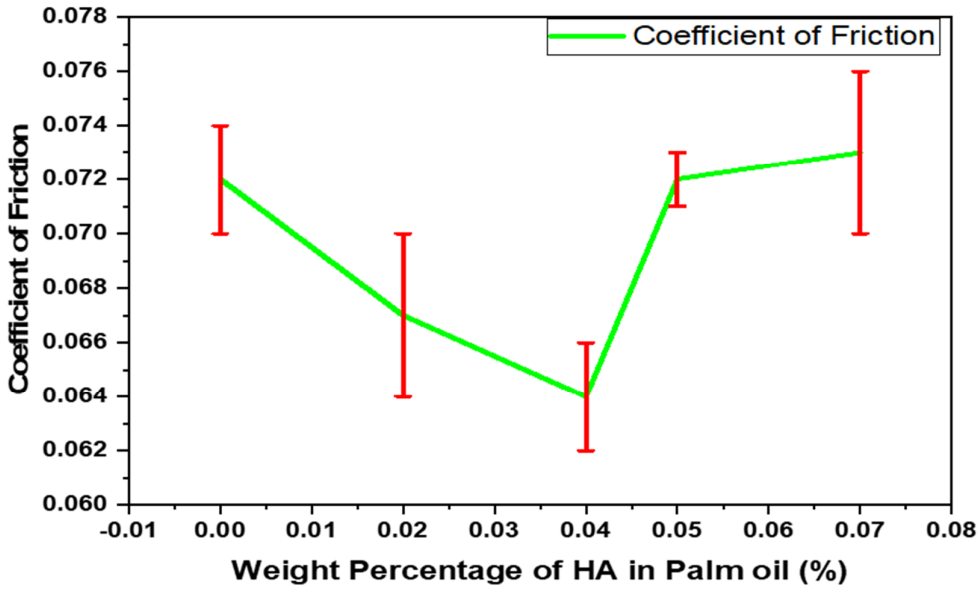

Fig. 9 – The coefficient of friction for different weight percentages of hydroxyapatite nanoparticles

10.

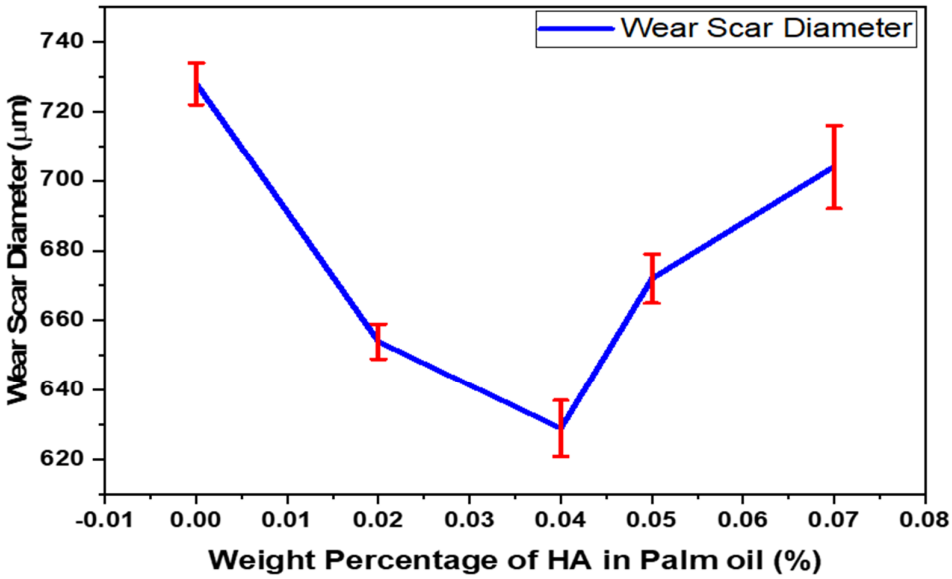

Fig. 10 – The wear scar diameter for different weight percentages of hydroxyapatite nanoparticles

11.

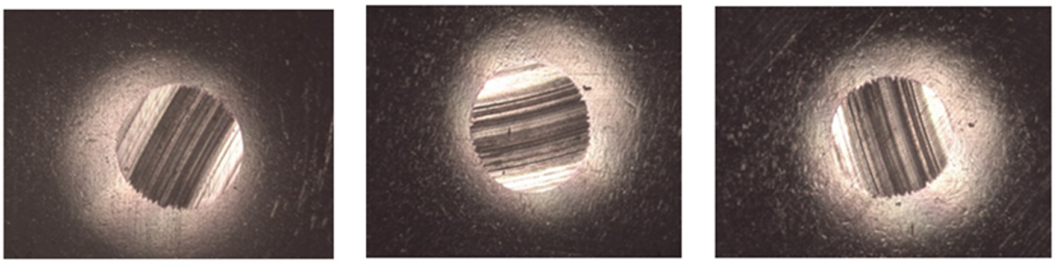

Fig. 11 – The wear scar diameter for palm oil sample

12.

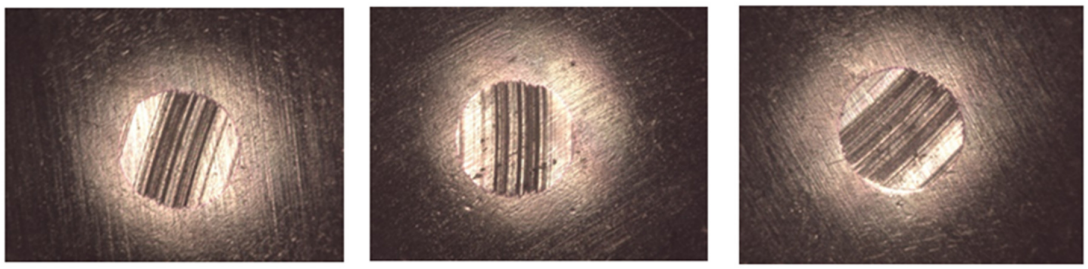

Fig. 12– The wear scar diameter for palm oil containing 0.04 % of hydroxyapatite nanoparticles

13.

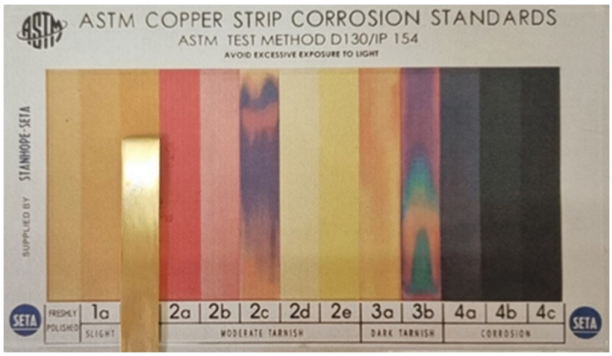

Fig. 13 – The copper strip immersed in palm oil containing 0.04 % of hydroxyapatite nanoparticles

Supplementary materials

Graphical Abstract